Available online at www.sciencedirect.com
ScienceDirect
Synthetic Metals 156 (2006) 1368–1377
SYNTHETIC METALS
www.elsevier.com/locate/synmet

EPR study of charge transfer in polyaniline highly doped by *p*-toluenesulfonic acid

V.I. Krinichnyi [a,*], S.V. Tokarev [a], H.-K. Roth [b], M. Schrödner [b], B. Wessling [c]

[a] *Institute of Problems of Chemical Physics, N.N. Semenov Avenue 1, Chernogolovka 142432, Russia*
[b] *TITK Institute Rudolstadt, Physical Materials Research, Breitscheidstrasse 97, Rudolstadt D-07407, Germany*
[c] *Ormecon GmbH, Ferdinand-Harten-Strasse 7, Ahrensburg D-22926, Germany*

Received 20 December 2005; received in revised form 11 September 2006; accepted 27 October 2006
Available online 18 December 2006

Abstract

Magnetic, relaxation and electronic dynamic parameters of paramagnetic centers in crystalline domains of polyaniline highly doped by *p*-toluenesulfonic acid (PANI-PTSA) as well as PANI-PTSA dispersed in poly(methyl methacrylate) were studied by the 3 cm (9.7 GHz) and 2 mm (140 GHz) wavebands EPR. These centers demonstrate the Lorentzian single line with the Dysonian contribution at both wavebands indicating intrinsic conductivity of metal-like domains near 1500–4000 S/cm at room temperature. Effective conductivity of the polymer is defined by Q3D delocalization of charge carriers within such domains and their Mott variable range hopping between the domains dominating its micro- and macroscopic conductivity. It was shown that the interaction of the charge carriers with the lattice phonons governs intradomain charge transfer at high temperatures. Reversible dipolare interaction of paramagnetic centers with oxygen was revealed. This interaction depends on electron precession frequency and/or on the PANI-PTSA dispersion in an insulating matrix. Charge transfer in PANI-PTSA was analyzed to be non-correlated with spin relaxation and dynamics that evidences the formation of Q3D metal-like domains contrary to the "single conducting chain" model.

Keywords: EPR; Polyaniline; Polaron; Relaxation; Dynamics

1. Introduction

Doped polyaniline (PANI-ES, the emeraldine salt form) and its derivatives possess high conductivity and are characterized by unusual spectroscopic and magnetic properties, attributed to the stabilization of polarons [1]. In highly doped polymers, a part of polarons can merge into diamagnetic bipolarons possessing two elemental charges. In contrast to other conducting polymers, the presence of the nitrogen nuclear in the PANI backbone stipulates the phenyl rings rotation near the polymer main *X*-axis and, therefore, leads to unique properties of this polymer. Two main conceptions of charge transfer in doped PANI are now considered. The first one considers elemental charge transfer along and between solitary polymer chains by polaron possessing spin $S = 1/2$ [2,3]. However, Kivelson and Heeger suggested [4] that interchain interaction in highly doped conducting polymers could suppress the Peierls instability and avoid 1D localization [5,6] due to significant interchain coherence. According to the alternative approach [7–9], polymer doping leads to the increase in its amorphous phase in number and size of more ordered metal-like domains with strongly coupled chains, in which the polarons are localized and charge is transferred by quasi-three-dimensional (Q3D) delocalized electrons. This approach points out that electronic and dynamic properties of the polymer are defined mainly by Q3D intradomain and Q1D interdomain charge transfer. Such a system is considered as a "Fermi glass", in which the electronic states at the Fermi energy ε_F are localized due to disorder and charge is transferred by the phonon-assisted Mott variable range hopping (VRH) between exponentially localized states near the Fermi level [10] in framework of the modified Drude model [11]. According to this model, electrons are accelerated by the applied electric field and lose their momentum through scattering by impurities and phonons. As a result of an electron's quantum diffusion an intrinsic conductivity of the Q3D domains should be near 10^7 S/cm, however, the experimental value does

* Corresponding author. Tel.: +7 496 522 1714; fax: +7 496 515 5420.
E-mail address: kivi@cat.icp.ac.ru (V.I. Krinichnyi).

0379-6779/$ – see front matter © 2006 Elsevier B.V. All rights reserved.
doi:10.1016/j.synthmet.2006.10.008

not exceed 10^3 S/cm [12]. Thus, there appears to be a mechanism in the polymers that can diminish even the intrinsic scattering of carriers by thermally excited phonons that limits the conductivity of good metals. The most plausible mechanism for this suppression of scattering by phonons in metallic regions is the Q1D conduction along polymer chains [4]. According to this approach, carriers can be scattered only back along the chains that requires phonons of relatively high energy, which do not exceeds $k_BT \approx 0.026$ eV (here k_B is the Boltzmann constant) below room temperature. Hence, conductivity should drop rather sharply at temperatures corresponding to $2k_F$, where k_F is the Fermi wavevector. Charge carriers resonantly tunnel between the domains through the strongly localized states in amorphous media [9,13].

PANI doped with *para*-toluene sulfonic acid (PANI-PTSA) and its dispersion in poly(methyl methacrylate) (PANI-PTSA/PMMA) yield the density of states at the Fermi level ε_F, $n(\varepsilon_F) \sim 10$–20 states per eV per two rings [14,15], that is an order of magnitude greater as compared with the value obtained for PANI-ES with other counterions. As PANI-PTSA is dispersed in PMMA, the Ph–N–Ph dihedral angle in PANI-ES domains with an averaged diameter of 8 nm decreases by 32° that leads to the increase in DC conductivity σ_{DC} [14]. Intrinsic conductivity and the mechanism of charge transfer in these metal-like domains has not been studied so far.

The polarons in conducting polymers are characterized by electron spin $S = 1/2$. Thus, the comparatively low-frequency ($\omega_e/2\pi = \nu_e \leq 10$ GHz) [16] and especially high-frequency ($\nu_e = 140$ GHz) [17] EPR methods are widely used for the study of such systems. Higher spectral resolution and sensibility of the latter allowed us to study various magnetic and electronic properties of different conducting polymers [17], PANI among them [18,19].

Javadi et al. showed [20] the stabilization of mobile and localized polarons in polymer phases with different crystallinity. Exposure to oxygen affect their magnetic and relaxation parameters due to dipole–dipole interaction with the oxygen biradicals each possessing total spin $S = 1$. It was found [21–23] that oxygen can reversibly broad the EPR spectrum of PANI without remarkable change in its conductivity. However, Kang et al. showed [24] that the air treatment of hydrochloric acid-doped PANI reversibly and simultaneously broadens its EPR spectrum and decreases its DC conductivity. Such changes were explained by the decrease in polarons mobility as a result of their interaction with the air. However, the opposite effect, i.e. the simultaneous broadening of the EPR spectrum and the rise in DC conductivity of the same air-treated polymer was reported by Houze and Nechtschein [25].

We present the first detailed results on the investigation of magnetic, relaxation and electronic transport properties of a crystalline phase in PANI-PTSA and PANI-PTSA/PMMA mainly by 3 cm and 2 mm wavebands EPR in a wide temperature range. Strong changes in these properties were shown at the polymer exposure to air. The nature of charge carries is analyzed and the mechanism of charge transfer is determined from the comparison of experimental data. Spin relaxation and dynamics was analyzed to be non-correlated with charge transfer processes that contradict the model of "single conducting chains" in PANI-ES [3,26] and justifies the formation of the Q3D metal-like domains in heavily doped PANI-PTSA. Previous results on the EPR study of PANI-PTSA have briefly been reported previously [27].

2. Experimental

Powder-like Ormecon® PANI-PTSA$_{0.5}$ with the lattice constants $a = 0.44$ nm, $b = 0.60$ nm, and $c = 1.10$ nm [28] was used. This sample was dispersed in PMMA using an appropriate technique under shear condition in melt phase. The volume fraction of PANI-PTSA was 30% in PANI-PTSA/PMMA as estimated from the X-ray measurements. These powders with a characteristic size R of individual particles of 0.0129 ± 0.0014 mm (PANI-PTSA) and 0.098 ± 0.006 mm (PANI-PTSA/PMMA) were mixed with MgO powder (1:3) and then placed into a quartz capillary with the inside diameter of ca. 0.6 mm. Such polymer dilution by an insulating matrix allowed one to avoid possible interaction between its powder particles and additionally to use Mn^{2+} with $g_{eff} = 2.00102$ and $a = 87.4$ G to determine g-factor as well as for the magnetic field sweep scale calibration at the 2 mm waveband EPR. For the analysis of the effect of air on magnetic resonance properties of PC, both vacuum-processed and nitrogen filled, and air-containing polymers were studied.

EPR experiments were performed using mainly 3 cm ($\nu_e = 9.7$ GHz) waveband PS-100X and 2 mm ($\nu_e = 140$ GHz) waveband EPR-05 spectrometers, both with 100 kHz field AC modulation for phase-lock detection. The 3 cm and 2 mm wavebands EPR spectra of nitrogen- and air-treated samples were registered in the temperature range of 120–320 K and their 3 cm waveband EPR spectra were also registered at 77 K in liquid nitrogen. The total spin concentration in the samples was determined using a $Cu_2S0_4 \cdot 5H_2O$ single crystal standard. Total paramagnetic susceptibility of the samples was determined using double integration of their EPR absorption spectra. EPR spectra were simulated using the Microcal Origin V.7.0552 and Bruker WinEPR SimFonia V.1.25 programs. The uncertainty in the determination of the peak-to-peak linewidth ΔB_{pp} and the value of g-factor was consequently $\pm 2 \times 10^{-2}$ G and $\pm 2 \times 10^{-4}$ at 3 cm waveband EPR and $\pm 5 \times 10^{-2}$ G and $\pm 3 \times 10^{-5}$ at 2 mm waveband EPR.

DC conductivity of the pellet-like samples was measured at 6–300 K using a four-probe technique.

3. Results and discussion

3.1. Dysonian term in EPR spectrum

The nitrogen-treated PANI-PTSA and PANI-PTSA/PMMA samples at 3 cm waveband EPR demonstrate Lorentzian exchange-narrowed lines with asymmetry factor A/B (the ratio of intensities of the spectral positive peak to negative one) of 1.03 and 1.25, respectively (Fig. 1). The exposure of the samples to air was observed to lead to the reversible line broadening and the increase in the asymmetry factor up to 1.27 and 1.42, respectively. The asymmetry of the EPR lines may arise due to either unresolved anisotropy of the g-factor or the presence of the

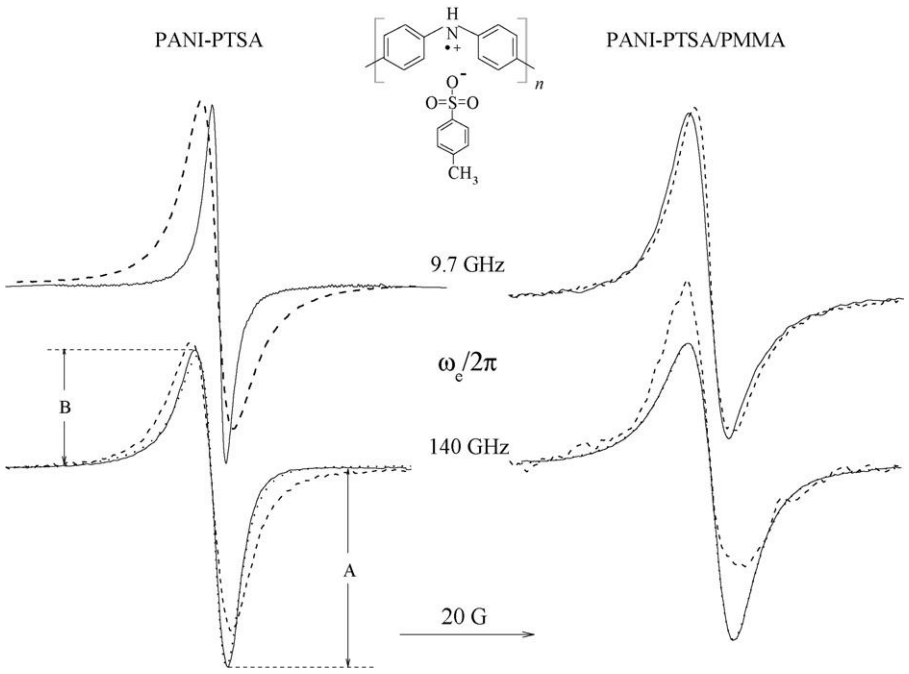

Fig. 1. A 3 cm and 2 mm wavebands EPR spectra of PANI-PTSA and PANI-PTSA/PMMA samples in nitrogen (solid lines) and air (dashed lines) atmosphere. The dotted lines show the spectra calculated from Eq. (1) with $D/A = 0.52$, $\Delta B_{pp} = 4.23$ G (left) and $D/A = 0.29$, $\Delta B_{pp} = 7.98$ G (right).

Dyson term [29] in the spectrum as a result of the interaction of microwave field with charge carriers inside the skin-layer with the thickness δ. To verify these assumptions, the 2 mm waveband EPR spectra of the samples were recorded. It is seen from Fig. 1, that the polymers in this waveband EPR also display a single asymmetric Lorentzian line, whose asymmetry factor increases from 1.68 up to 1.95 (PANI-PTSA) and from 1.46 up to 1.78 (PANI-PTSA/PMMA) on the exposition to air. This fact indicates a substantial interaction of PC even in high fields, the line asymmetry of these PC indeed results from the interaction of microwave field with the charge carriers inside the skin layer. PC with the Dysonian line shape are commonly registered in different highly doped conducting polymers [16,17], PANI among them [18,19,30,31]. Such line shape distortion is accompanied by the line shift into higher magnetic fields and the drop of sensitivity of EPR technique. This implies that to determine more correctly and complete such main magnetic resonance parameters as g-factor, peak-to-peak linewidth ΔB_{pp} and paramagnetic susceptibility, one should calculate Dysonian spectra of PC in PANI.

Generally, the Dyson line consists of absorption A and dispersion D terms; therefore, one can write the following equation for its first derivative:

$$\frac{d\chi}{dB} = A\frac{2x}{(1+x^2)^2} + D\frac{1-x^2}{(1+x^2)^2} \quad (1)$$

where $x = (B - B_0)/\Delta\omega_L$, B_0 the resonant magnetic field, $\Delta\omega_L = 1/T_2\gamma_e$ the Lorentzian single line width, T_2 the spin–spin relaxation time, and γ_e is the hyromagnetic ratio for electron. The analysis showed that the parameters A and B of the line asymmetry shown in Fig. 1 correlated with the coefficients A and D of Eq. (1) as $A/B = 1 + 1.45D/A$.

Some EPR spectra calculated using Eq. (1) are displayed in Fig. 1 by dotted lines. The calculation of the spectra presented in Fig. 1 allowed one to determine an effective g-factor for PC in the nitrogen- and air-treated PANI-ES to be equal to 2.00280 and 2.00274, respectively. These values are lower then those obtained for PC localized on six carbon atoms and one nitrogen atom in the repeating unit arising a shift of g-factor of free electron, $g_e = 2.00232$, up to $g \approx 2.0031$ and to $g \approx 2.0054$, respectively [32], so the spins in the polymers under study are delocalized over some repeating units each with the size of ca. 0.5 nm. This gives a lower limit of the localization length of electrons in the samples.

3.2. Spectra linewidth

The temperature dependence of the effective absorption peak-to-peak linewidth ΔB_{pp} of the samples determined at both the 3 cm and 2 mm wavebands EPR are given in Fig. 2. ΔB_{pp} measured at 3 cm waveband for PANI-PTSA lies near that obtained for the PANI highly doped with hydrochloric acid [20]. It is seen that this value increases not more than by a factor of two as ν_e increases from 9.7 up to 140 GHz. Such insignificant line broadening with the operating frequency increase was not observed in the studies on other conducting polymers [16,17], including PANI [18,19,30]. This may be evidence of a stronger exchange interaction between PC in the polymers under study, which is neither partly nor completely relieved in strong magnetic fields. The linewidth of PC in the PANI-PTSA sample containing nitrogen slightly depends on temperature. At the dispersion of this polymer in PMMA, its linewidth becomes sensitive to temperature (Fig. 2). Air diffusion into the samples leads to the reversible extremal broadening of their

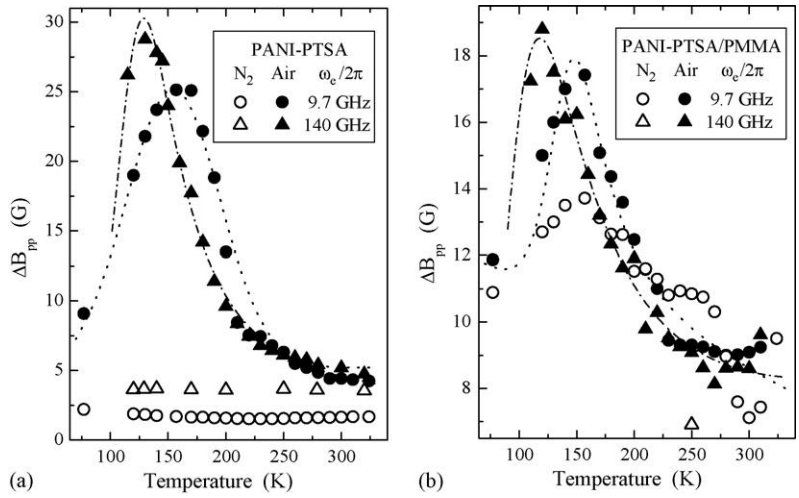

Fig. 2. Temperature dependence of linewidth of PC in PANI-PTSA (a) and PANI-PTSA/PMMA (b) samples filled by nitrogen (open points) and air (filled points) registered at different wavebands EPR. The lines show the dependences calculated from Eq. (2) with $\omega_{lib}^0 = 9.6 \times 10^{17}$ s^{-1}, $E_a = 0.058$ eV, $J = 0.28$ eV (dash–dotted line), $\omega_{lib}^0 = 1.3 \times 10^{19}$ s^{-1}, $E_a = 0.102$ eV, $J = 0.36$ eV (dotted line) (a) and with $\omega_{lib}^0 = 5.8 \times 10^{15}$ s^{-1}, $E_a = 0.031$ eV, $J = 0.015$ eV (dash–dotted line), $\omega_{lib}^0 = 8.1 \times 10^{17}$ s^{-1}, $E_a = 0.090$ eV, $J = 0.041$ eV (dotted line) (b).

EPR line characterized by the critical point T_c (Fig. 2). The increase in the linewidth at the polymer dispersion suggests less motional narrowing [33] and hence, increased localization of PC in PANI-PTSA/PMMA.

The contact of the PANI-ES with the air leads to reversible broadening of its EPR line and also to the extremal temperature dependency of the ΔB_{pp} value with the characteristic temperature T_c (Fig. 2). At the increase of the polarizing frequency from 9.7 up to 140 GHz this value determined for PANI-PTSA and PANI-PTSA/PMMA is shifted from 160 to 130 K and from 150 to 120 K, respectively. These effects can probably be described in terms of the Houze–Nechtschein approach [25] postulating the dipole–dipole interaction of the polarons hopping along the solitary polymer chains with the fixed oxygen molecules possessing total spin $S = 1$. The collision of both types of spins should additionally broaden the absorption EPR line by the value

$$\delta(\Delta\omega) = p\omega_{hop}C = \frac{16}{27}\omega_{hop}C\left(1 + \frac{\hbar^2\omega_{hop}^2}{144J^2}\right) \quad (2)$$

where p is the flip–flop probability during a collision of both spins, ω_{hop} the frequency of the polaron hopping along a polymer chain, C the number of oxygen molecules per each aniline ring equal to 0.005 for PANI [25], $\hbar = h/2\pi$ the Plank constant, and J is the constant of the spin dipole–dipole interaction in the system. If the ratio $J/\hbar$ exceeds the frequency of collision of both types PC, then the condition of strong interaction is realized in the system leading to direct relation of the spin–spin interaction and polaron diffusion frequencies, so then $\lim[\delta(\Delta\omega)] = 16/27\, C\omega_{hop}$. In an opposite case the condition of weak interaction prevails in the system resulting for an inverse dependence of these frequencies, $\lim[\delta(\Delta\omega)] = 4/3\,(C/\omega_{hop})(J/\hbar)^2$. According to the spin exchange fundamental concepts [34] the extremal character of the $\delta(\Delta\omega)$ temperature dependency should evidence the realization of both types of spin–spin interaction at $T \leq T_c$ and $T \geq T_c$, respectively. One more reason for the line broadening can be spin localization with the temperature decrease at $T \geq T_c$.

The growth of interaction between the solitary polymer chains in heavily doped PANI causes their transformation into crystalline metal-like domains with localized polarons and Q3D delocalized electronic wave functions [7,9,35]. Therefore, to use this approach we should assume the dipole–dipole interaction of the localized polarons with adsorbed oxygen molecules librating near the polymer chains. Such initial conditions make it possibly to apply the chain of argument in the Houze–Nechtschein theory for the interpretation of our data.

Supposing an activation character of small-scale librations of the oxygen molecules near polymer chains with frequency $\omega_{hop} = \omega_{lib} = \omega_{lib}^0 \exp(-E_a/k_BT)$ the $\Delta B_{pp}(T)$ dependencies presented in Fig. 2 were fitted well by Eq. (2) with $E_a = 0.058$ eV, $J = 0.28$ eV and $E_a = 0.102$ eV, $J = 0.36$ eV (Fig. 2a), and with $E_a = 0.031$ eV, $J = 0.015$ eV and $E_a = 0.090$ eV, $J = 0.041$ eV (Fig. 2b). The J values determined sufficiently exceed an appropriate constant of spin collision of nitroxide radicals with paramagnetic ions in liquids, $J \leq 0.01$ eV [34]. The dispersion of the initial PANI-PTSA sample in PMMA leads to the decrease in both the J and E_a values. These values additionally decrease with the increase of the registration frequency. Such effects can probably be explained, e.g. by the effect of an external magnetic field on the spin exchange process in the polymers under study. The decrease in T_c with the increase of the external magnetic field seems to justify this supposition.

3.3. Paramagnetic susceptibility

Paramagnetic susceptibility determined using double integration of the absorption term A of nitrogen- and air-treated PANI samples are shown in Fig. 3 as a function of temperature. Generally, this parameter of spin reservoir consists of the temperature dependent Curie contribution χ_C of the spins

localized in amorphous regions of polymer and temperature independent one of the Pauli spins, χ_P

$$\chi_{pm} = \chi_C + \chi_P = \frac{N_s \mu_{eff}^2}{3k_B T} + \mu_{eff}^2 n(\varepsilon_F), \quad (3)$$

where $N_e\mu_{eff}^2/3k_B = C$ is the Curie constant, N_s the spin volume density, $\mu_{eff} = \mu_B g\sqrt{S(S+1)}$ the effective magneton, μ_B the Bohr magneton, and $n(\varepsilon_F)$ is the density of states at the Fermi level ε_F.

In the free-electron model, the slope and the intercept of the χT versus T plot yield Pauli susceptibility and the Curie constant, respectively. The C and $n(\varepsilon_F)$ values were determined for the nitrogen-treated PANI-PTSA and PANI-PTSA/PMMA samples to be 1.3×10^{-3} emu K/mol, 0.69 states/(eV 2 Ph) and 1.9×10^{-2} emu K/mol, 4.8 states/(eV 2 Ph), respectively, at room temperature. Effective paramagnetic susceptibility of both PANI samples increases considerably at their exposure to air (Fig. 3). This effect can probably be explained by the decay of part of diamagnetic bipolarons into polarons due to the formation of >NH···•O–O•···HN< bridges with hydrogen bonds, which can act as spin traps in air-treated PANI [36]. It should be noted that the extremal temperature dependence of χ shown in Fig. 3 complicates a separate determination of the terms of Eq. (3) and may lead to deviation in $n(\varepsilon_F)$ obtained by the magnetic resonance and, e.g. heat-capacity [37] methods.

3.4. Spin relaxation and dynamics

The nitrogen and oxygen nuclei possess own magnetic momentum, and their hyperfine interaction with electrons should lead to the broadening of the EPR line. As a result of such interaction between electron and proton with magnetic momentum μ_p separated by distance r, the linewidth of PANI should be $\Delta B = \mu_p/r \approx 14$ G. However, the linewidth of the nitrogen containing sample is nearly one order magnitude smaller probably due to mobility of charge carriers, which averages superfine electron–proton interaction [38].

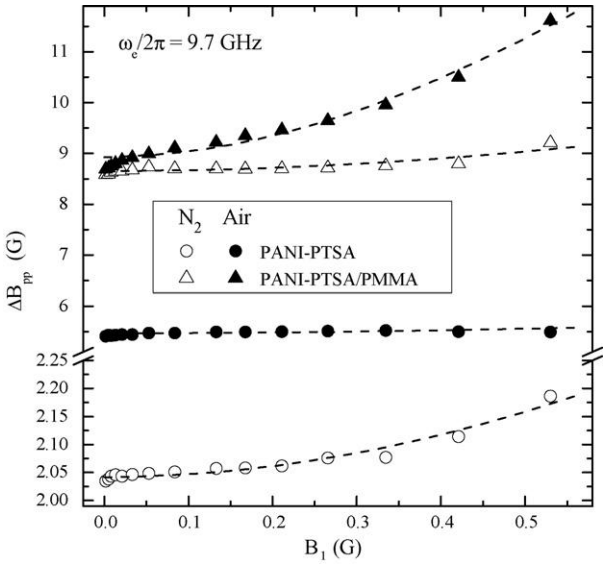

Fig. 4. Peak-to-peak linewidth ΔB_{pp} of PC in PANI-PTSA and PANI-PTSA/PMMA samples as function of the term B_1 of the microwave polarizing field. Top–down dashed lines display the dependences calculated from Eqs. (4a) and (4b) with $B_1 = 0.53$ G and, respectively, $\Delta B_{pp}^{(0)} = 8.92$ G, $T_1 = 1.1 \times 10^{-6}$ s, $T_2 = 7.4 \times 10^{-9}$ s, $\Delta B_{pp}^{(0)} = 8.68$ G, $T_1 = 1.4 \times 10^{-7}$ s, $T_2 = 7.6 \times 10^{-9}$ s, $\Delta B_{pp}^{(0)} = 5.27$ G, $T_1 = 1.1 \times 10^{-7}$ s, $T_2 = 1.6 \times 10^{-8}$ s, $\Delta B_{pp}^{(0)} = 2.08$ G, $T_1 = 1.2 \times 10^{-7}$ s, $T_2 = 3.1 \times 10^{-8}$ s.

As the microwave magnetic component B_1 increases, the absorption line of PC is broadened as it is seen in Fig. 4. Such steady-state saturation of the spin reservoir allows one to determine the effective spin–lattice T_1 and spin–spin T_2 relaxation times of PC from relations [39]

$$T_1 = \frac{4[(\Delta B_{pp}/\Delta B_{pp}^{(0)})^2 - 1]}{\gamma_e^2 B_1^2 T_2} \quad (4a)$$

$$T = \frac{\sqrt{3}}{2\gamma_e \Delta B_{pp}^{(0)}} \quad (4b)$$

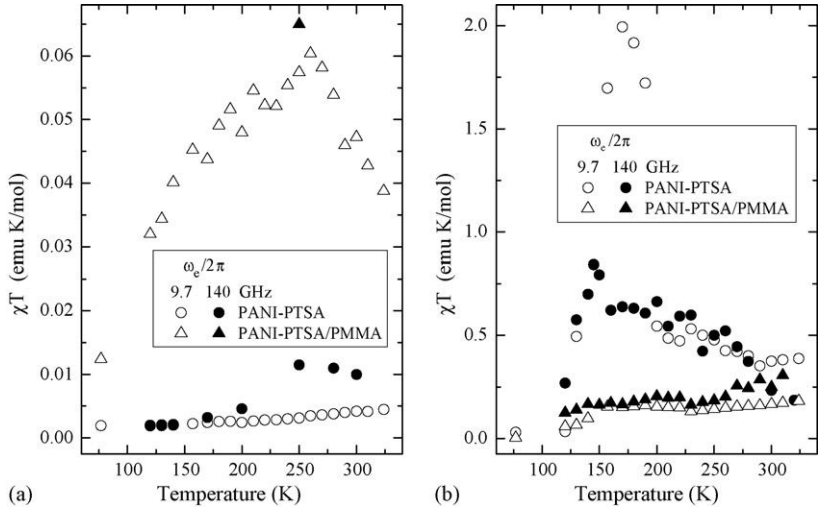

Fig. 3. Temperature dependence of the χT product of PC in nitrogen- (a) and air- (b) treated PANI-PTSA and PANI-PTSA/PMMA samples determined at $\omega_e/2\pi = 9.7$ GHz (open symbols) and $\omega_e/2\pi = 140$ GHz (filled symbols).

Table 1
Spin–lattice (T_1) and spin–spin (T_2) relaxation times (in s), spin intrachain (D_{1D}) and interchain (D_{3D}) diffusion rates (in rad/s), conductivity due to hypothetical intrachain (σ_{1D}) and interchain (σ_{3D}) polaron mobility (in S/cm) (the conductivity terms due to joint polaron and bipolaron mobility are presented below the respective values calculated for polarons) as well as the intrinsic conductivity (σ_{AC}, in S/cm) determined from Dysonian EPR spectra for the initial and dispersed PANI samples at $\omega_e/2\pi = 9.7$ GHz and room temperature

Sample	T_1	T_2	D_{1D}	D_{3D}	σ_{1D}	σ_{3D}	σ_{AC}
PANI-PTSA[a]	1.2×10^{-7}	3.1×10^{-8}	9.0×10^{7}	1.7×10^{7}	6.3×10^{-5} 1.1×10^{-2}	3.6×10^{-6} 6.4×10^{-4}	1460
PANI-PTSA[b]	1.1×10^{-7}	1.6×10^{-8}	1.9×10^{11}	5.3×10^{6}	6.7 24.2	5.5×10^{-5} 2.0×10^{-4}	4100
PANI-PTSA/PMMA[a]	1.4×10^{-7}	7.6×10^{-9}	1.9×10^{9}	7.2×10^{5}	5.4×10^{-3} 0.24	6.1×10^{-7} 2.7×10^{-5}	120
PANI-PTSA/PMMA[b]	1.1×10^{-6}	7.4×10^{-9}	1.4×10^{12}	1.1×10^{4}	13.6 178	3.2×10^{-8} 4.2×10^{-7}	210

[a] In nitrogen atmosphere.
[b] In air atmosphere.

where $\Delta B_{pp}^{(0)}$ is the linewidth of unsaturated line at the $B_1 \to 0$ limit and γ_e is the hyromagnetic ratio for electron. The relaxation parameters of PC determined using such a method are presented in Table 1.

If the polarons can really diffuse even in highly doped PANI [3] along and between the polymer chains with respective diffusion coefficients D_{1D} and D_{3D}, they should induce an additional magnetic field in the whereabouts of another spins leading to the acceleration of electron relaxation of the whole spin ensemble. As the relaxation times of the spin reservoir is defined mainly by a dipole–dipole interaction between the spins, the following equations can written [40]:

$$T_1^{-1}(\omega_e) = \langle\omega^2\rangle[2J(\omega_e) + 8J(2\omega_e)] \quad (5a)$$

$$T_2^{-1}(\omega_e) = \langle\omega^2\rangle[3J(0) + 5J(\omega_e) + 2J(2\omega_e)] \quad (5b)$$

where $\langle\omega^2\rangle = 1/10\gamma_e^4\hbar^2 S(S+1)n\Sigma_{ij}$ is the constant of a dipole–dipole interaction for powder, n a number of polarons per each monomer, Σ_{ij} the lattice sum for powder-like sample, $J(\omega_e) = (2D_{1D}^{|}\omega_e)^{-1/2}$ at $D_{1D}^{|} \gg \omega_e \gg D_{3D}$ or $J(0) = (2D_{1D}^{|}D_{3D})^{-1/2}$ at $D_{3D} \gg \omega_e$ a spectral density function for Q1D motion, $D_{1D}^{|} = 4D_{1D}/L^2$, ω_e the resonant angular frequency of the electron spin precession, and L is a factor of spin delocalization over a polaron. The similar spectral density function was earlier used in the study of spin dynamics in PANI [18,19,30] and other conducting polymers [16,17].

The conductivity of a polymer due to so supposed Q1D and Q3D mobility of N_p polarons, each transferring e elemental charge, can be determined as

$$\sigma_{1D,3D} = \frac{N_p\ e^2 D_{1D,3D} d_{1D,3D}^2}{k_B T}, \quad (6)$$

where $d_{1D,3D}$ are corresponding lattice constants.

Both coefficients of hypothetical polaron diffusion in PANI as well as the respective components of the polymer conductivity due to such PC mobility calculated from Eqs. (5a) and (5b) at $L \approx 5$ [41] and Eq. (6), respectively, are presented in Table 1 as well. The data show that as PANI-PTSA sample contacts with air, the anisotropy of the spin diffusion D_{1D}/D_{3D} and conductivity σ_{1D}/σ_{3D} increases approximately by four orders of magnitude. These ratios additionally increase by an order of magnitude at the dispersion of the initial sample in PMMA. This implies that the exposure of PANI-ES to air and/or its dispersion in PMMA should lead to higher spin delocalization along the polymer chain.

If one supposes the existence of double charged diamagnetic bipolarons additionally to polarons moving with the diffusing coefficients calculated for polarons, the respective effective conductivities can also be evaluated (see Table 1).

3.5. DC conductivity

Fig. 5 shows that DC conductivity of the PANI-PTSA and PANI-PTSA/PMMA samples non-monotonously changes with

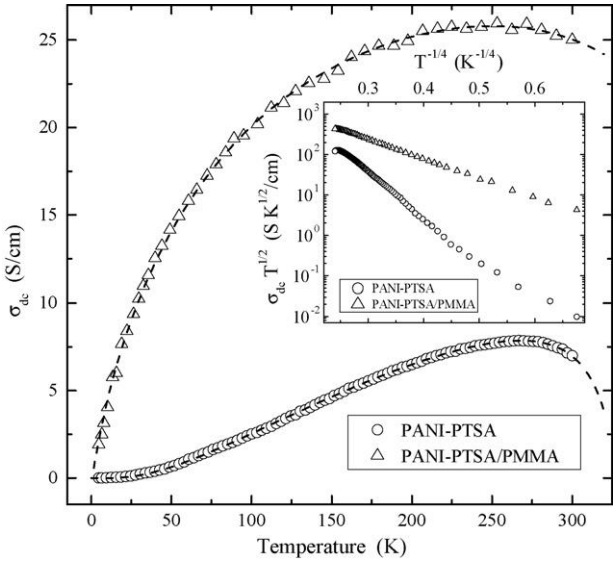

Fig. 5. DC conductivity σ_{DC} vs. T and $\sigma_{DC}T^{1/2}$ vs. $T^{-1/4}$ (insert) of PANI-PTSA and PANI-PTSA/PMMA samples. Top–down lines display the dependences calculated from Eq. (9) with $k_1 = 3.4 \times 10^{-3}$ S/cm, $k_2 = 0.86$ S/cm K, $T_0^* = 1500$ K, $d = 3$, $\hbar\omega_{ph} = 0.032$ eV and $k_1 = 1.3 \times 10^{-2}$ S/cm, $k_2 = 1.8$ S/cm K, $T_0^{|} = 1140$ K, $d = 1$, and $\hbar\omega_{ph} = 0.025$ eV, respectively.

temperature as it is typical for granular metals [8]. The analysis of the low-temperature branch of the $\sigma_{DC}(T)$ dependence of both the PANI-PTSA and PANI-PTSA/PMMA samples exposed on air allows one to suppose a realization of the Mott Q1D and Q3D VRH charge transfer through less conducting (disordered, amorphous) regions typical for granular metal [42]. According to this model, the conductivity of the system with dimension d depends on temperature as [43]

$$\sigma_{DC}(T) = \sigma_0 \ \exp\left[-\left(\frac{T_0^{|,*}}{T}\right)^{1/d+1}\right] \tag{7}$$

where $\sigma_0 = 2\pi\, e^2\omega_0 n(\varepsilon_F) b^2 t_0 \tau_i/h^2 s$, $T_0^{|} = 16/[k_B n(\varepsilon_F) z\langle L\rangle]$ at $d=1$ and $T_0^{*} = 16/[k_B n(\varepsilon_F)\langle L\rangle^3]$ at $d=3$ [44] the characteristic temperature, above which conductivity is essentially defined by the phonon bath, and below which conductivity is defined by the distributional disorder of electron states in space and energy, ω_0 the upper hopping frequency nearly equal to optical phonon frequency, ω_{ph}, t_0 the transfer integral equal to 2–3 eV for π-electron, z a number of the nearest neighbor chains equal to four for PANI [43], $\langle L\rangle$ the average length of the charge carrier wave function (or localization length), b the interchain separation, t_0 the interchain charge transfer integral, τ_i the mean free time, and s is the average chain cross-sectional area.

The heating of the samples above 270 K leads to the decrease in σ_{DC} (Fig. 5). For explanation of this phenomenon the Kivelson–Heeger model of charge carrier scattering on optical lattice phonons proposed for the interpretation of charge transfer in metal-like domains in π-conjugated polymers [4] seems to be more suitable. According to this model, intrinsic conductivity of domains depends on temperature as

$$\sigma_{int}(T) = \sigma_0 T\left[\sinh\left(\frac{\hbar\omega_{ph}}{k_B T}\right) - 1\right] \tag{8}$$

where $\sigma_0 = N_e\ e^2c^2Mt_0^2k_BT/8\pi\hbar^3\alpha^2$, N_e the volume density of carriers with elemental charge e, c the lattice constant, M the mass of NH group, and α is the electron–phonon interaction constant equal, for example, to 4.1×10^8 eV cm^{-1} for *trans*-polyacetylene [4].

Therefore, effective conductivity σ_{DC} can be described by a superposition of Eqs. (7) and (8) with appropriated coefficients k_1 and k_2

$$\sigma_{DC}^{-1}(T) = k_1\ \exp\left[\left(\frac{T_0^{|,*}}{T}\right)^{1/d+1}\right] + k_2T^{-1}\left[\sinh\left(\frac{\hbar\omega_{ph}}{k_BT}\right) - 1\right]^{-1} \tag{9}$$

Fig. 5 shows that the experimental data obtained for PANI-PTSA and PANI-PTSA/PMMA samples exposed to air are fitted well by Eq. (9) with $T_0^{|} = 1140$ K, $d=1$, $\hbar\omega_{ph}=0.025$ eV and $T_0^{*} = 1500$ K, $d=3$, $\hbar\omega_{ph}=0.032$ eV, respectively. At the dispersion of the PANI-PTSA sample in PMMA its $n(\varepsilon_F)$ value increases from 3 up to 17 states/(eV 2 Ph) [15]. This is accompanied by the appropriate decrease of the charge localization length from 14 down to 1.5 nm. The latter value does not exceed the effective radius of the metal-like domain in PANI-PTSA equal to 4 nm [45]. Assuming respective Q1D and Q3D VRH in the nitrogen-treated samples, one can determine the analogous decrease in their $\langle L\rangle$ from 59 down to 2.3 nm.

The form of Eq. (9) evidences that two successive charge transfers through two regions with lower and higher crystallinity are explicitly realized in the polymers. The most probable distance of the charge carrier hopping in air-containing PANI-PTSA, $R = 1/4(T_0/T)^{1/2}\ \langle L\rangle$ [43] is 6.8 nm at room temperature. In the framework of the Q1D VRH model the energy of the charge carrier hopping in metal $W = 1/2\, k_B(T_0T)^{1/2}$ [43] should be near k_BT [42]. W was calculated for the PANI-PTSA studied to be 0.025 eV at room temperature lying near $k_BT \approx 0.026$ eV. The velocity of charge carrier, $v_F = 2c/\pi\hbar n(\varepsilon_F)$ [43] near the Fermi energy level, $\varepsilon_F = 3N_e/2n(\varepsilon_F)$ [46], were determined to be $v_F = 3.7\times10^7$ cm s^{-1} and $\varepsilon_F = 0.79$ eV. The Fermi velocity determined is approximately the same (3×10^7 cm s^{-1}) as obtained for highly doped polymer [47], whereas the latter value lies near the Fermi energy obtained for PANI doped by camphorsulfonic (0.4 eV) [48] and sulfuric (0.5 eV) [18] acids. Taking the mean free path l_i equal to the coherency length in PANI 4 nm [49], we estimated $\tau_i = 1.3\times10^{-13}$ s. The R and W values calculated for Q3D VRH of charge carriers in PANI-PTSA/PMMA are [42,43] $R = [9\langle L\rangle/8\pi k_BTn(\varepsilon_F)]^{1/4} = 1.5$ nm and $W = k_B(T_0T^3)^{1/4}/2 \approx 0.019$ eV.

The anisotropy of Q1D VRH charge transfer, i.e. the ratio of mobilities of charge carriers along and between polymer chains, is [43]

$$\frac{\sigma_{||}}{\sigma_\perp} = \frac{\langle L\rangle}{2k_BTzn(\varepsilon_F)b^2} \tag{10}$$

The anisotropy of DC conductivity $\sigma_{||}/\sigma_\perp$ was determined from the experimental data to decrease from ca. 60 down to 1.2 as the dimensionality d increased from 1 up to 3 at the PANI-PTSA dispersion in PMMA. The $\langle L\rangle$ values obtained are much greater than the interchain distance in the samples that allows one to point out the 3D character of the metallic states in both the PAN-ES studied. We propose that similarly to PANI with other counterions [7,18,19,30,35], PAN-ES in PANI-PTSA also appears as a Q1D disordered conductor, which consists of bundles of strongly coupled parallel chains, in which electron wave functions are Q3D delocalized, different from conventional 1D conductors based on organic ion-radical salts [50,51]. The formation of such bundles is attributed to significant interchain coherence [4] as well as interchain coupling [52] that disagrees with the "single conducting chain" models of PAN-ES [3,26].

3.6. AC conductivity

Intrinsic conductivity σ_{AC} and the mechanism of charge transfer in PANI with doping level lying above the percolation threshold depend on the structure and number of counterions introduced into a polymer. At high doping level the saturation of spin-packets decreases significantly due to the increase in direct and cross spin–spin and spin–lattice interactions. Normally, the Dysonian term appears in EPR spectra of such polymers due to

the formation of a skin-layer on their surface. The shape of the Dysonian EPR line is obviously defined by intrinsic conductivity of the sample, σ_{AC}, that enables one to determine directly this value within a skin-layer from its EPR spectrum. In contrast to the saturated dispersion EPR signal, the Dyson-like line shape "feels" dynamics of spin polaron and spinless bipolaron charge carriers diffusing through a skin layer. Since the number and dynamics of each type of charge carriers can differ, electronic dynamic properties of the sample should depend on its doping level.

If the skin-layer with thickness δ is formed on the spherical surface with radius R and conductivity σ_{AC}, coefficients A and D in Eq. (1) can be calculated from equations [53]

$$\frac{4A}{9} = \frac{8}{p^4} - \frac{8(\sinh p + \sin p)}{p^3(\cosh p - \cos p)} + \frac{8\ \sinh p\ \sin p}{p^2(\cosh p - \cos p)^2} + \frac{\sinh p - \sin p}{p(\cosh p - \cos p)} - \frac{\sinh^2 p - \sin^2 p}{(\cosh p - \cos p)^2} + 1 \tag{11a}$$

$$\frac{4D}{9} = \frac{8(\sinh p - \sin p)}{p^3(\cosh p - \cos p)} - \frac{4(\sinh^2 p - \sin^2 p)}{p^2(\cosh p - \cos p)^2} + \frac{\sinh p + \sin p}{p(\cosh p - \cos p)} - \frac{2\ \sinh p\ \sin p}{(\cosh p - \cos p)^2} \tag{11b}$$

where $p = 2R/\delta$ and $\delta = (2/\omega_e\sigma_{AC})^{1/2}$. In the case of $\sigma_{AC} \to 0$ or $\delta \to \infty$ typical for insulator its dispersion term becomes equal to zero, and Eq. (1) is transformed to a simple equation for the first derivative of a symmetrical absorption signal.

Fig. 6 shows the σ_{AC} versus T dependences calculated for the PANI-PTSA and PANI-PTSA/PMMA samples using Eq. (1) and Eqs. (11a) and (11b) at different polarizing frequencies. Room temperature intrinsic conductivity of the nitrogen-treated PANI-PTSA and PANI-PTSA/PMMA samples lies near 1000–1500 S/cm and 40–120 S/cm, respectively, and weakly depend on temperature (Fig. 6). As the polymers contact with air, these values increase remarkably (see Table 1) and become more temperature dependent. In contrast to PANI doped with other counteriones, –NH– fragments in the PANI-PTSA are more accessible for own microenvironment. So, the conductivity can possibly be changed due to formation of >NH···$^{\bullet}$O–O$^{\bullet}$···HN< bridges with hydrogen bonds that increases a probability of interchain charge transfer. It should be noted that these values sufficiently exceed σ_{1D} and σ_{3D} above calculated supposing Q1D polaron or/and bipolaron diffusion along the "single conducting chain". Further to this approach one should expect $\Delta B_{pp}(T) \propto T_2^{-1}(T) \propto \sigma_{AC}(T)$ (see Eq. (4b) and Eq. (5b)) for the polymers exposed to air. It is seen, however, that the linewidth demonstrate extremal temperature behavior, whereas the σ_{AC} value changes rather monotonically, at least in a high temperature range. Such an extremal shape of the $\Delta B_{pp}(T)$ can, therefore, be explained by the reversible dipole–dipole interaction of localized PC with the oxygen molecules activative librating near the polymer chains assumed above. Such a discrepancy in the $\Delta B_{pp}(T)$ and $\sigma_{AC}(T)$ shapes refutes Q1D charge transfer and justifies the formation of metal-like domains with localized polarons and Q3D delocalized charge carriers in the PANI samples. As in the case of PANI doped with other counterions [18], charge dynamics in the samples under study can be interpreted in the frames of the most widely used pair approximation [54] that gives for Q3D charge hopping [42]

$$\sigma_{AC}(T) = \frac{e^2 n^2(\varepsilon_F)\langle L\rangle^3 k_B T\omega_e}{96s}\ \ln^4\frac{\omega_{ph}}{\omega_e} = \sigma_0 T \tag{12}$$

Fig. 6 shows that AC conductivity determined experimentally for PANI-PTSA/PMMA exposed to air and PANI-PTSA containing nitrogen or air from their Dysonian EPR spectra follows well Eq. (12), at least in a high temperature range. Conductivity determined for both samples at 140 GHz was surprisingly lower than that determined at lower frequency. This is possibly due to a deeper penetration of microwave quant with higher energy into the polymer bulk. In this case the σ_{AC} obtained should be

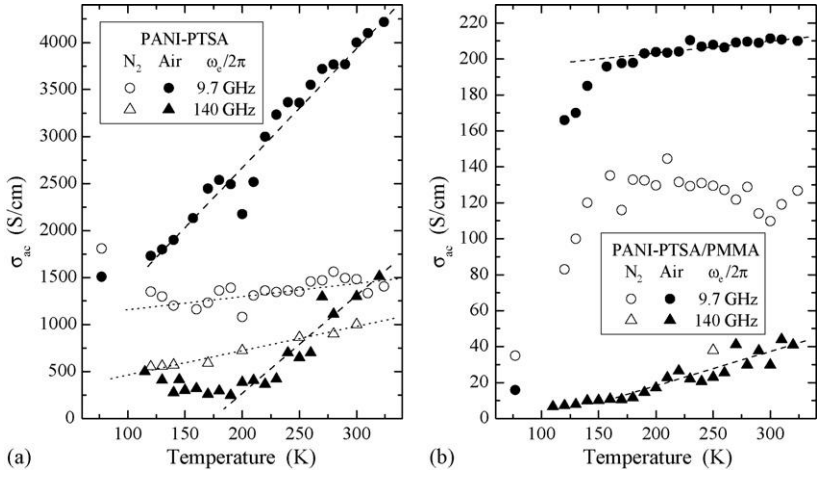

Fig. 6. Temperature dependence of AC conductivity of PANI-PTSA (a) and PANI-PTSA/PMMA (b) samples in nitrogen (open symbols) and air (filled symbols) atmosphere determined from their Dysonian spectra registered at different wavebands EPR. Top–down dotted lines in (a) present the dependences calculated from Eq. (12) with $\sigma_0 = 2.0$ S/cm K and $\sigma_0 = 2.6$ S/cm K, respectively. By the top–down dashed lines are shown the dependences calculated from Eq. (12) with, respectively, $\sigma_0 = 12.3$ S/cm K and $\sigma_0 = 9.3$ S/cm K (a) and $\sigma_0 = 0.087$ S/cm K and $\sigma_0 = 0.17$ S/cm K (b).

rated as a lower limit of intrinsic conductivity at this waveband EPR.

Intrinsic conductivity was calculated for the PANI-PTSA and PANI-PTSA/PMMA samples from Eq. (12) with $\omega_e/2\pi = 9.7$ GHz and $s = 0.05$ nm^2 to be 4.3×10^3 S/cm and 290 S/cm, respectively. These values lie close to those calculated from the Dysonian EPR spectra of these samples (see Table 1). However, these values calculated from Eq. (12) for the air containing samples with $n(\varepsilon_F) = 3$ and 17 states/(eV 2 Ph) [15] should be equal to 6.8×10^4 S/cm and 3.1×10^3 S/cm, respectively, that is more than an order of magnitude higher than those presented in Table 1.

4. Conclusions

Multifrequency EPR study of the initial and dispersed PANI-PTSA samples allowed to determine their relaxation, conformation and charge dynamics properties. These properties are defined mainly by the formation in PANI-ES of Q3D high crystalline metal-like domains with significant interchain coherence. The polarons are localized in such domains due to a strong interaction between the neighboring conducting chains. In contrast to other conducting polymers, the interaction between polarons in PANI-ES does not reduced at magnetic field up to 5 T. The formation of metallic domains in PAN-ES is attributed to the significant interchain interaction in the ordered crystalline regions, which avoids Q1D localization. Disordering effects existing in the polymer transform the metallic state characteristic of ideal polymer chains with completely delocalized electrons into the 'Fermi glass' with finite density of states at the Fermi level. Conductivity of the pure PANI-PTSA sample was defined to be governed by Q3D intradomain and Q1D interdomain charge transfer and the latter is characterized by charge transfer through the regions with different crystallinity. Charge transport in PANI-PTSA dispersed in an insulating polymer matrix is defined by Q3D inter- and intradomain hopping. The dispersion of initial PANI-PTSA leads to the formation of quasi-metallic domains with a broad 3D energy band and 3D interrelated delocalized electrons surrounded by disordered matrix. This results in less effective AC conductivity as compared to pure PANI-PTSA and possibly decreases the height of amorphous barriers. In this system a charge Q3D tunnels from particle to particle through an insulating barrier. PMMA layer hampers the penetration of air to metal-like domains additionally decreasing their intrinsic conductivity. Such a picture agrees with the mesoscopic nanometal concept pointed out polyaniline as granular metal in which the dispersion induced insulator-to-metal transition, however, contradicts the "single conducting chain" models of PAN-ES.

The presence of air near >NH fragments reduces electrostatic Coulomb interaction between positive charges on the PANI-PTSA chains and the anions, and, thus, increases delocalization of spins (not polarons as quasi-particles) over the polymer backbone. Besides, the bridges with hydrogen bonds are formed in PANI-ES filled with air that result in the increase in its intrinsic conductivity. The dipole–dipole interaction of polarons with the oxygen molecules leads to reversible changes in spin relaxation and depends on the intensity of an external magnetic field. The interaction between these PC decreases with the polymer dispersion in an insulating matrix, and is accompanied with the decrease in the activation energy of spin–spin collisions and in the energy transfer from a spin reservoir to a polymer lattice.

Acknowledgements

We would like to thank Dr. N.N. Denisov for assistance at EPR experiment. This work was in part supported by the Russian Foundation for Basic Researches, Grants Nos. 03-03-04005 and 05-03-33148.

References

[1] D.C. Trivedi, in: H.S. Nalwa (Ed.), Handbook of Organic Conductive Molecules and Polymers, vol. 2, John Wiley, Chichester, 1997, pp. 505–572 (Chapter 12).
[2] Y. Cao, P. Smith, A.J. Heeger, Synth. Met. 32 (1989) 263.
[3] K. Mizoguchi, M. Nechtschein, J.-P. Travers, C. Menardo, Phys. Rev. Lett. 63 (1989) 66.
[4] S. Kivelson, A.J. Heeger, Synth. Met. 22 (1988) 371.
[5] V.N. Prigodin, Y.A. Firsov, JETP Lett. 38 (1983) 284.
[6] V.N. Prigodin, Y.A. Firsov, W. Weller, Solid State Commun. 59 (1986) 729.
[7] A.G. MacDiarmid, A.J. Epstein, Faraday Disc. 88 (1989) 317.
[8] A.B. Kaiser, Adv. Mater. 13 (2001) 927.
[9] V.N. Prigodin, A.J. Epstein, Europhys. Lett. 60 (2002) 750.
[10] P.W. Anderson, Commun. Solid State Phys. 2 (1970) 193.
[11] K. Lee, A.J. Heeger, Synth. Met. 84 (1997) 715.
[12] J. Joo, E.J. Oh, G. Min, A.G. MacDiarmid, A.J. Epstein, Synth. Met. 69 (1995) 251.
[13] V.N. Prigodin, A.J. Epstein, Synth. Met. 125 (2001) 43.
[14] B. Wessling, H.S. Nalwa (Eds.), Handbook of Organic Conductive Molecules and Polymers, vol. 3, John Wiley & Sons, Chichester, 1997, pp. 497–632 (Chapter 11).
[15] A. Raghunathan, P.K. Kahol, J.C. Ho, Y.Y. Chen, Y.D. Yao, Y.S. Lin, B. Wessling, Phys. Rev. B 58 (1998) R15955.
[16] K. Mizoguchi, S. Kuroda, in: H.S. Nalwa (Ed.), Handbook of Organic Conductive Molecules and Polymers, vol. 3, John Wiley & Sons, Chichester, New York, 1997, pp. 251–317 (Chapter 6).
[17] V.I. Krinichnyi, in: S. Schlick (Ed.), Advanced ESR Methods in Polymer Research, John Wiley & Sons Inc., New York, 2006, pp. 307–338 (Chapter 12).
[18] V.I. Krinichnyi, H.-K. Roth, G. Hinrichsen, F. Lux, K. Lüders, Phys. Rev. B 65 (2002) 155205.
[19] V.I. Krinichnyi, S.D. Chemerisov, Y.S. Lebedev, Phys. Rev. B 55 (1997) 16233.
[20] H.H.S. Javadi, R. Laversanne, A.J. Epstein, R.K. Kohli, E.M. Scherr, A.G. MacDiarmid, Synth. Met. 29 (1989) E439.
[21] A. Bartle, L. Dunsch, H. Naarmann, D. Schmeisser, W. Gopel, Synth. Met. 61 (1993) 167.
[22] K. Aasmundtveit, F. Genoud, E. Houze, M. Nechtschein, Synth. Met. 69 (1995) 193.
[23] P.K. Kahol, A.J. Dyakonov, B.J. McCormick, Synth. Met. 84 (1997) 691.
[24] Y.S. Kang, H.J. Lee, J. Namgoong, B. Jung, H. Lee, Polymer 40 (1999) 2209.
[25] E. Houze, M. Nechtschein, Phys. Rev. B 53 (1996) 14309.
[26] D.S. Galvao, D.A. don Santos, B. Laks, C.P. de Melo, M.J. Caldas, Phys. Rev. Lett. 63 (1989) 786.
[27] V.I. Krinichnyi, S.V. Tokarev, H.-K. Roth, M. Schrödner, B. Wessling, Synth. Met. 152 (2005) 165.
[28] B. Wessling, D. Srinivasan, G. Rangarajan, T. Mietzner, W. Lennartz, Eur. Phys. J. E 2 (2000) 207.
[29] F.J. Dyson, Phys. Rev. B 98 (1955) 349.

[30] A.L. Kon'kin, V.G. Shtyrlin, R.R. Garipov, A.V. Aganov, A.V. Zakharov, V.I. Krinichnyi, P.N. Adams, A.P. Monkman, Phys. Rev. B 66 (2002) 075203.
[31] D. Srinivasan, T.S. Natarajan, G. Rangarajan, S.V. Bhat, B. Wessling, Solid State Commun. 110 (1999) 503.
[32] J.R. Morton, Chem. Rev. 64 (1964) 453.
[33] R. Kubo, K. Tomita, J. Phys. Soc. Jpn. 9 (1954) 888.
[34] Y.N. Molin, K.M. Salikhov, K.I. Zamaraev, Spin Exchange, Springer, Berlin, 1980.
[35] F. Zuo, M. Angelopoulos, A.G. MacDiarmid, A.J. Epstein, Phys. Rev. B 36 (1987) 3475.
[36] B.Z. Lubentsov, O.N. Timofeeva, S.L. Saratovskikh, V.I. Krinichnyi, A.E. Pelekh, V.V. Dmitrenko, M.L. Khidekel, Synth. Met. 47 (1992) 187.
[37] P.K. Kahol, Phys. Rev. B 62 (2000) 13803.
[38] N.M. Atherton, Electron Spin Resonance, Wiley, New York, 1973.
[39] Ch.P. Poole, Electron spin resonance, in: A Comprehensive Treatise on Experimental Techniques, John Wiley & Sons, New York, 1983.
[40] F. Carrington, A.D. McLachlan, Introduction to Magnetic Resonance with Application to Chemistry and Chemical Physics, Harrer & Row, Publishers, New York, Evanston, London, 1967.
[41] F. Devreux, F. Genoud, M. Nechtschein, B. Villeret, in: H. Kuzmany, M. Mehring, S. Roth (Eds.), Electronic Properties of Conjugated Polymers, Springer Series in Solid State Sciences, vol. 76, Springer-Verlag, Berlin, 1987, pp. 270–276.
[42] N.F. Mott, E.A. Davis, Electronic Processes in Non-crystalline Materials, Clarendon Press, Oxford, 1979.
[43] Z.H. Wang, A. Ray, A.G. MacDiarmid, A.J. Epstein, Phys. Rev. B 43 (1991) 4373.
[44] E.P. Nakhmedov, V.N. Prigodin, A.N. Samukhin, Sov. Phys. Solid State 31 (1989) 368.
[45] R. Pestler, G. Nimtz, B. Wessling, Phys. Rev. B 49 (1994) 12718.
[46] J.S. Blakemore, Solid State Physics, Cambridge University Press, Cambridge, 1985.
[47] K. Lee, M. Reghu, E.L. Yuh, N.S. Sariciftci, A.J. Heeger, Synth. Met. 68 (1995) 287.
[48] K.H. Lee, A.J. Heeger, Y. Cao, Phys. Rev. B 48 (1993) 14884.
[49] M.E. Jozefowicz, R. Laversanne, H.H.S. Javadi, A.J. Epstein, J.P. Pouget, X. Tang, A.G. MacDiarmid, Phys. Rev. B 39 (1989) 12958.
[50] J.M. Williams, J.R. Ferraro, R.J. Thorn, K.D. Carlson, U. Geiser, H.H. Wang, A.M. Kini, M.-H. Whangboo, Organic Superconductors (Including Fullerenes): Synthesis, Structure, Properties and Theory, Prentice-Hall Inc., Englewood Cliffs, New Jersey, 1992.
[51] Z. Todres, Organic Ion Radicals. Chemistry and Applications, Marcel Dekker, New York, 2002.
[52] Y.A. Firsov, in: H. Fritzsche, D. Adler (Eds.), Localization and Metal Insulator Transition, Plenum, New York, 1985, p. 471.
[53] A.C. Chapman, P. Rhodes, E.F.W. Seymour, Proc. Phys. Soc., B 70 (1957) 345.
[54] A.R. Long, Adv. Phys. 31 (1982) 553.